Ab initio study of H_2O and water-chain-induced properties of carbon nanotubes

B. K. Agrawal, V. Singh, A. Pathak, and R. Srivastava
Physics Department, Allahabad University, Allahabad 211002, India
(Received 27 November 2006; revised manuscript received 26 March 2007; published 16 May 2007)

We perform an *ab initio* study of the motion of the nano sized water dimer through a single-walled carbon nanotube (SWCNT), the stability of an encapsulated one-dimensional (1D) water chain inside SWCNT, and the H_2O-induced structural, energetic, electronic, and optical properties of the SWCNTs. The adsorption of the water molecules is caused by the dispersion forces, i.e., the van der Waals (vdW) interactions. Thus, the role of the vdW interactions in the estimation of the BE for the weakly bound adsorbates cannot be ignored as has been done in several earlier publications. We find that a single H_2O molecule or single water dimer or a 1D chain of water dimers is trapped inside the medium-sized (6,6) carbon nanotube placed in vacuum. However, the H_2O molecule or water dimer may be transmitted in case the tube is surrounded by water or water vapor at high vapor pressure at high temperatures. On the other hand, a chain of single H_2O molecules or more number of the encapsulated H_2O molecules is very weakly coupled to the wide (10,10) carbon nanotube and can, thus, easily transmit through the carbon nanotube in agreement with the recent experiments. Further, appreciable adsorption both inside and on the surface of the (10,10) carbon nanotube is predicted in concurrence with the experiments. The small (medium-sized) diameter tubes will adsorb strongly (accommodate) the water molecules outside (inside) the nanotubes. The H_2O adsorption converts the conducting small-diameter zigzag (5,0) tube into a semiconductor. Further, the adsorption reduces the band gap of the semiconducting achiral zigzag (10,0) nanotube but increases the band gap of a chiral semiconducting (4,2) tube. The adsorbed H_2O molecules increase the electrical conductivity in agreement with the experiment. The overall peak structure in the optical absorption for the pristine tube is not altered significantly by the adsorption except for small alterations in the energy locations and the relative intensities of the peaks in the achiral tubes.

DOI: 10.1103/PhysRevB.75.195421 PACS number(s): 78.67.Ch, 73.21.−b, 61.48.+c, 81.05.Tp

I. INTRODUCTION

Any phenomenon related with the water has a unique place because of its importance in our daily life. The adsorption of the water molecules on the carbon nanotubes is of immense interest for many reasons. In many membrane-spanning transport proteins, water-filled pores having sizes similar to the nanotubes, e.g., aquaporines and the ion channels, are present. Aquaporines create water-permeable pores in several cell membranes,[1] whereas the ion channels produce ion-permeable pores.[2] These pores determine the electrical properties of the nerve cells.

By employing molecular-dynamics simulations, Hummer *et al.*[3] have observed pulselike transmission of water through a finite-sized (6,6) carbon nanotube immersed in a water reservoir for an assumed strength of the carbon-water interaction and also sharp two-state transitions between empty and filled states on a nanosecond time scale for the reduced strength of this interaction. The nanotubes may thus be used as unique molecular channels for H_2O and proton, with the channel occupancy and conductivity tunable by changes in the local channel polarity and solvent conditions.

The two-state transitions between empty and filled states may help in understanding the crystallographically empty but functionally filled hydrophobic channels in the proton-transferring proteins.[4] The water influx can be triggered by the changes in the amino-acid ionization states for obtaining the protonic connectivities. The excitation of the covalently bonded dye molecules by light could drive the emptying and/or filling transitions in the membrane-inserted functionalized nanotubes, which may have applications in the generation of the light sensors as single-molecule field-effect transistors for protonic currents.[3]

The basic physics of the phenomenon of the adsorption of atoms or molecules on the nanotubes needs to be understood. One should know (i) the geometries and the types of bonding between the adsorbant and the nanotube, (ii) the effects of the adsorption on the physical properties of the nanotubes, and (iii) how the diameter and chirality of the tube determine the new physical properties.

The adsorption affects most of the physical properties of the single-walled carbon nanotubes (SWCNTs). There may be quite useful applications such as gas storage,[5,6] electronic and thermal properties,[7–9] field emission,[10] biotechnology,[11] catalysis, differential absorption, nanowire and nanotube production,[12,13] etc. The fabrication of very thin wires and tubes within controllable sizes is possible by employing SWCNTs as templates. These products have practical applications as conducting connect in nanodevices based on molecular electronics. As a source of hydrogen, a camera flash can generate hydrogen by splitting of water confined in carbon nanotubes.[14] There may be adsorption inside the SWCNTs (endohederal) or on the surfaces (exohederal) or at the grooves or the interstitial channels of the bundles of SWCNTs.

Very recently, the rapid flow of water through large-diameter (of 13–20 Å) carbon nanotubes has been reported.[15,16]

Some calculations[17,18] for determining the water-graphite or water-carbon interactions for their use in molecular-dynamics simulations have been performed. The effects of the range and orientational dependence of the potentials have been emphasized.

A number of the adsorption measurements[19–21] and NMR (Ref. 22) experiments have been done to study the adsorption of the various inert atoms or molecules such as Xe, N, CH_4, C_2H_6, etc., on the carbon nanotubes and nanoropes.

In the literature, some theoretical calculations at different levels on the adsorption of the H_2O molecules[3,23–27] on or inside the carbon nanotubes are available. Hummer *et al.*[3] observed pulselike transmission of water through a finite-length short uncapped SWCNT of length 13.4 Å and diameter 8.1 Å immersed in a water reservoir. The tube contained about five water molecules for 66 ns. Gordillo and Marti[23] noted a decrease in the hydrogen bonds when the water is confined in the nanotubes. Walther *et al.*,[24] investigated some structural properties of water surrounding a carbon nanotube. Later on, Gordillo and Marti[25] studied H_2O adsorption on the outer surface of a bundle of (10,10) carbon nanotubes by employing molecular-dynamics simulations and the phenomenological intramolecular interactions. They observed adsorption inside the grooves formed by the tubes in the low-concentration region and a first-order transition in the high-concentration region leading to adsorption on the available surface. Zhao *et al.*[26] used an *ab initio* method to study a number of gases adsorbed on SWCNTs and bundles and observed that most of the molecules are adsorbed quite weakly. The above *ab initio* calculations have limitations for the following reasons: Firstly, the local-density approximation (LDA) of the density-functional theory (DFT) was used. As the results obtained for such systems in the LDA and in the generalized gradient approximation (GGA) have earlier been seen to be quite different,[28,29] one should also study these systems in the GGA to know the real situation. Secondly, they ignored the dispersion forces or the van der Walls (vdW) interactions that have been reported to be quite significant in the weakly bound systems.[28–30] In addition, the zero-point energy was not considered. Also, all the calculations are available only for the large-diameter nanotubes, and the study of the small-diameter nanotubes is not available. We have tried to address the above points in the present investigation.

We perform an *ab initio* study of (a) the motion of a H_2O molecule and also a water dimer containing two H_2O molecules obeying approximately the well-known ice rules through a carbon nanotube, (b) the infinitely long one-dimensional (1D) chains of H_2O molecules and water dimers inside the infinitely long carbon nanotube, and (c) the adsorption of the H_2O molecules on the various adsorption sites of the small-diameter 4 Å SWCNTs and the large-diameter nanotubes of different types. We investigate how the curvature of the nanotubes affects the adsorption of the H_2O molecules. A fully self-consistent pseudopotential method using the DFT in GGA as well as in LDA has been employed. We also consider the contributions of the vdW energy as well as the zero-point energy.

Earlier, we have successfully employed the above method for the investigation of the various physical properties of the nanotubes doped by the donor Li atoms[31] and the inert Xe atoms[28] and CH_4 molecules.[29]

II. METHOD AND TECHNICAL DETAILS

For the details of the LDA and GGA methods, we refer to the accompanying article.

The DFT method in GGA or LDA considers only the short-range interactions, namely, the chemical ones. The weak long-range vdW interactions or the dispersion forces between the H_2O molecule and the carbon nanotube need to be considered. We also consider the H_2O-H_2O molecular vdW interaction energy wherever needed.

We determine the total attractive vdW interaction energy for a system using the expression

$$Et_{\mathrm{vdW}} = -\sum_i \sum_j C_{ij}\left(\frac{1}{r_{ij}}\right)^6. \tag{1}$$

Here, the units of C_{ij} are energy $\times$ (distance)[6] and the subscripts i, j stand either for the different H_2O molecules present in a carbon nanotube or the H_2O molecule and the C atoms in a H_2O-doped carbon nanotube. In order to estimate the contribution of vdW energy to the binding energies, one should determine this vdW energy for one H_2O molecule, i.e., $E_{\mathrm{vdW}}=Et_{\mathrm{vdW}}/n$, where Et_{vdW} is given by Eq. (1), and n is the number of the H_2O molecules in a system.

To obtain the vdW interactions between the H_2O and H_2O molecules, and that between the H_2O molecule and the C of the CNT, we employ the C_{ij}'s as given by Halgren.[32] The combination relation within Slater-Kirkwood approximation is used. For the H_2O–carbon tube vdW interaction, C_{ij} is seen to be 800.83 eV (au).[6] On the other hand, for the H_2O-H_2O molecular vdW interaction energy, we obtain C_{ij} = 1234.58 eV (au).[6] In all the results of the present paper, we have always included the vdW interaction energies. The convergence of the vdW energy has been checked by including more and more atoms for the infinitely long nanotubes.

For a reliable quantitative estimate of the binding energy at 0 K, one needs to include the entropy contribution, which is the total zero-point vibrational energy (ZPVE) for a system given by

$$Et_{\mathrm{zp}} = \frac{1}{2}\sum_i \hbar\omega_i. \tag{2}$$

Here the sum extends over all the phonon frequencies (ω_i) for all the atoms in a unit cell of the system. Here, both the rotational and librational vibrations are considered.

In the actual calculation of the final binding energy, one has to consider the ZPVE per molecule, E_{zp}, which is given by $E_{\mathrm{zp}}=Et_{\mathrm{zp}}/n$, where n is the number of the H_2O molecules per unit cell.

In order to understand the coupling or binding of the H_2O molecules with the carbon nanotubes, we define a chemical binding energy per H_2O molecule, E_{CB}, by

$$E_{\mathrm{CB}} = [E(\mathrm{CNT}) + E(n\mathrm{H_2O}) - E(\mathrm{NT} + n\mathrm{H_2O})]/n, \tag{3}$$

where E(CNT) is the energy of the isolated carbon nanotube, $E(n\mathrm{H_2O})$ is the energy of the n number of the H_2O molecules in isolation, and $E(\mathrm{CNT}+n\mathrm{H_2O})$ is the combined energy of the carbon nanotube and the n number of the H_2O molecules. All the above energies are obtained per unit cell after optimizing the corresponding components or the full system. The E_{CB} is the chemical energy by which the energy of the tube is lowered by the doping of the H_2O molecules.

The final binding energy E_{FB} per H_2O molecule is given by

$$E_{FB} = E_{CB} + E_{vdW} - \Delta E_{zp}, \quad (4)$$

with E_{vdW} as the van der Waals energy and ΔE_{zp} as the enhanced ZPVE, ΔE_{zp}. The enhanced ZPVE, ΔE_{zp}, can be obtained by

$$\Delta E_{zp} = [E_{zp}(\text{DCNT}) - E_{zp}(\text{CNT}) - E_{zp}(n\text{H}_2\text{O})]/n, \quad (5)$$

where E_{zp}(DCNT) is the ZPVE for the unit cell of the carbon nanotube doped with n number of the H_2O molecules, E_{zp}(CNT) is the ZPVE of the pristine carbon nanotube per unit cell, and $E_{zp}(n\text{H}_2\text{O})$ is the ZPVE of the n number of the H_2O molecules in isolation.

The calculation of ΔE_{zp} in a doped carbon nanotube involves a tedious evaluation (involving quite large computer time) of the phonon-dispersion curves and density of phonon states for both the isolated and doped carbon nanotubes which is beyond the scope of the present study. We, therefore, adopt a simple method as described in the Appendix. We present the results for the enhanced ZPVE, ΔE_{zp}, obtained for the various H_2O–carbon nanotube configurations in Table IV.

It may be pointed out that the binding energies, here, are similar to the cohesive energies of the solids given in the literature. All the energies of a system including its components are negative, but the computed binding energies, here, are the differences between the negative energies according to their specific definitions as given by Eqs. (3)–(5).

A unit cell generates an infinitely extended linear chain parallel to the tube axis inside or outside it, and the nanotube works as a template for the fabrication of linear and/or zigzag chains or circular nanowires or nanotubes of the adsorbates.

III. CALCULATION AND RESULTS

A. Structural properties

A positive value of the E_{FB} favors the binding of the adsorbate with the carbon nanotube, whereas a negative E_{FB} means no binding of the adsorbate.

For any system, we relax both the lattice constants and the atomic positions in the unit cell simultaneously to achieve the minimum-energy atomic configuration. We observe that the E_{CB} depends both on the number of the chosen $\vec{k}$ points in the Brillouin zone (BZ) and the plane-wave cutoff energy. We obtain the convergence with respect to both these parameters. In several earlier publications, this criterion has been overlooked. The plane-wave cutoff energy was varied from 40 to 90 Ry, and for the convergence, a cutoff energy of 80 Ry was found to be sufficient. The E_{CB}'s were obtained for 2–8 $\vec{k}$ points chosen in the Monkhorst-Pack grid and we found that E_{CB} converges for four $\vec{k}$ points within 4%.

During optimization, in general, the Hellmann-Feynman forces were reduced to 10^{-2} eV/Å on each atom barring some cases where the forces were higher but less than 10^{-1} eV/Å. It may be noted that in an *ab initio* calculation, the above criterion is sufficient to achieve reliable results as has been widely accepted and reported in the literature.

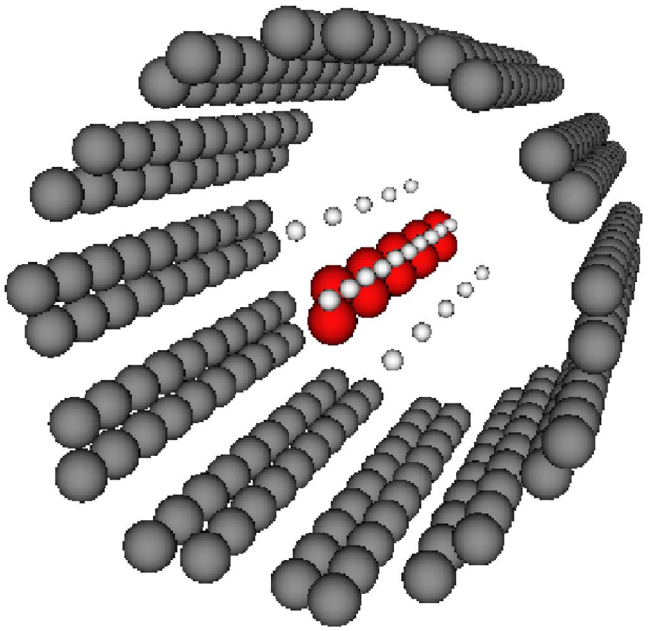

FIG. 1. (Color online) Actually calculated minimum-energy atomic configuration of a part of the optimized (6,6) carbon nanotube encapsulating water dimers, each dimer containing 2-H_2O molecules. The shaded circles denote the C atoms of the host (6, 6) carbon nanotube, the dark (red) circles represent the O atoms whereas the small open circles show the H atoms.

In order to avoid the interference effects between the neighboring H_2O molecules in the supercell geometries, appropriate vacuum space has been chosen. In all cases, a minimum separation of 40 Å between the walls of the neighboring images was chosen. The convergence was tested by increasing this separation between the images up to 50 Å and the results were seen to converge within 5%.

A single unit cell of the isolated (3,3), (5,0), (4,2), (6,6), (10,0), and (10,10) nanotubes contains 12, 20, 56, 24, 40, and 40 atoms, respectively. The number of atoms is enhanced in some specific systems.

In Fig. 1, we depict our actually calculated minimum-energy atomic configuration of a part of the optimized (6,6) carbon nanotube encapsulating water dimers, each dimer containing two H_2O molecules. The shaded circles denote the C atoms of the host (6,6) carbon nanotube, the dark (red) circles represent the O atoms, whereas the small open circles show the H atoms. On repetition along the tube axis, a unit cell forms an infinite 1D chain of the water dimers encapsulated inside the (6,6) carbon nanotube. This unit cell also represents the finite-sized (6,6) carbon nanotube through which the water dimer is moving, starting far from one end of the (6,6) carbon nanotube, entering the nanotube, and then moving away to a large distance from the other end of the tube. The present figure is drawn for a situation when the water dimer lies fully inside the (6,6) carbon nanotube.

At first, one finds out those sites on the surface of the carbon nanotube where the system has minimum energy with respect to its surroundings. These sites are the surface midhexagonal and the top sites. In the midhexagonal site, the

H_2O molecule resides above the middle of the hexagon formed by the six host C atoms of the carbon nanotube, whereas in the top site configuration, the H_2O molecule occupies a position just above a host C atom of the nanotube.

We optimize the orientation of the H_2O molecule to achieve the minimum energy at each of the minimum-energy site of the nanotube. The H_2O molecule is a planar molecule and this plane may be either parallel or normal to the tube axis. Further, the system energy may also depend on the rotation of the molecule about an axis parallel to the H-H axis or about an axis normal to its plane. During optimization, we have considered all such possibilities and determined the corresponding E_{FB}'s. There are three different orientations of the H_2O molecule with respect to the carbon nanotube. They are named as O atom toward the tube surface, 1-H atom toward the tube surface, and 2-H atoms toward the tube surface.

The calculated E_{CB}'s in GGA using the two commonly used exchange and correlation functionals such as those of Perdew *et al.*[33] (PBE) and of Becke *et al.*[34] have been seen to be quite close; we, therefore, use the PBE exchange-correlation functional in all our calculations.

Finally, as the H_2O molecule is a polar molecule, there are long-range dipole-dipole interactions. We have taken care of it in all our calculations. We perform all our computation for all the carbon nanotube–H_2O systems after selecting sufficient vacuum space between the images of the H_2O molecules and the carbon nanotube to avoid the interference effects between the images. The size of the supercell normal to the carbon nanotube axis is chosen as 41 Å and the convergence has been checked up to a size of 51 Å.

It may be pointed out that in the present study, all the considered systems are the infinitely extended carbon nanotubes containing infinitely extended H_2O molecular chains except stated otherwise.

As indicated earlier, one is interested in knowing the role of chirality on the adsorption of the H_2O molecules and the resulting physical properties. This study is not feasible for the large-diameter nanotubes because of the involved computation, but is possible only for the small-diameter nanotubes. We thus investigate these tubes here.

1. Small-diameter nanotubes

There are three types of the 4 Å diameter nanotubes. Among them, two are achiral armchair (3,3) and zigzag (5,0) nanotubes, and the third one is the chiral (4,2) tube. They are investigated to bring out the chirality-dependent effects. The optimized diameters of the pristine (5,0), (3,3), and (4,2) nanotubes are 4.10, 4.34, and 4.28 Å, respectively. The study is then extended to the larger-diameter nanotubes such as the (6,6), (10,0), and (10,10) tubes to elucidate the role of the curvature on the adsorption. The optimized diameters of the zigzag (10,0), armchair (6,6), and (10,10) nanotubes are seen to be 7.85, 8.19, and 13.49 Å, respectively.

The adsorption of the H_2O molecules on the nanotubes does not distort the adsorbate H_2O molecules themselves appreciably. The changes in the bond lengths and the bond angles in the H_2O molecules are quite small and lie within 5% and 1%, respectively. Also, the diameters of all the studied carbon nanotubes remain quite unchanged after the adsorption of the H_2O molecules.

The H_2O adsorption incurs a radial deformation all along the length of the nanotube. This radial deformation, named as buckling, is measured by the percentage of the difference between the maximum and minimum radii of the nanotube with respect to the averaged radius of the tube. We observe that the small-diameter tubes are buckled quite strongly as compared to the large-diameter tubes. However, for the most stable configurations, the buckling for the small-diameter tubes lie within 9%.

H_2O-doped (3,3) nanotube. A perusal of Table IV of the Appendix reveals that the computed enhanced ΔE_{zp} for the doped (3,3) tube is 20.9 meV. We have encapsulated the H_2O molecule inside the tube and found that the E_{FB} is negative and, therefore, the adsorption inside the tube is ruled out. The same will be true for the other 4 Å carbon nanotubes.

We study all the three different orientations of the H_2O adsorbed on the surface of the tube and observe that the E_{FB} is either negative or quite small that means no or small adsorption in the majority of the cases in GGA. The binding is caused mainly by the E_{vdW}. The highest E_{FB} of 0.087 eV is seen for the midhexagonal site having H_2O plane normal to the tube axis and the O atom toward the tube surface. It is noted that the corresponding E_{FB} calculated in LDA is high (0.181 eV). The E_{FB} for the H_2O molecule at the top site of the nanotube surface in GGA is 0.067 eV (0.064 eV) which is obtained when the H_2O plane is normal to the nanotube axis and one H (O) atom lies toward the surface of the carbon nanotube.

The unit cell contains 12 C atoms and the presence of one H_2O molecule will amount to a concentration of 8.3%. As a test case, we reduced this concentration to half (4.2%) for the midhexagonal site by optimizing a configuration where there is one H_2O molecule for two unit cells. The E_{FB} increases only by a few percent indicating the existence of a quite weak repulsive H_2O-H_2O interaction in the chain of the H_2O molecules. This is supported by the subsequent discussion.

We performed a separate calculation for an isolated 1D chain of the H_2O molecules and found an equilibrium separation of 2.89 Å between the H_2O molecules. In the (3,3) tube, the lattice constant along the tube axis is 2.39 Å, and as this separation of 2.39 Å between the two H_2O molecules along the chain is smaller than the corresponding above calculated equilibrium separation of 2.89 Å in isolation, there exists some positive (repulsive) contribution to the energy of the doped tube because of the H_2O-H_2O interactions. This adsorbate-adsorbate interaction vanishes for the low concentration of the H_2O molecules, e.g., for one H_2O molecule adsorbed on the two unit cells (24 C atoms) where the H_2O-H_2O separation in the chain becomes largely equal to 4.78 Å.

H_2O-doped (5,0) nanotube. The enhanced ΔE_{zp} is seen to be 12.5 meV both for the midhexagonal and top sites. The E_{FB}'s for the different adsorption sites are significant and larger than those seen for the armchair (3,3) nanotube. The preferred adsorption site is again the midhexagonal one followed by the top site. The binding is dominated by the vdW interaction. The highest E_{FB} (=0.113 eV) is obtained for the midhexagonal site having H_2O plane normal to the tube axis

TABLE I. Binding energy per H_2O molecule in eV for the adsorption of H_2O molecule in or on (6,6) nanotube in GGA. The final binding energy, $E_{FB}=E_{CB}+E_{vdW}-\Delta E_{zp}$ ($\Delta E_{ZP}=0.025$ eV). The averaged diameter of the carbon nanotube and the separation between O and the nearest C of SWCNT in Å and the bucklings are also included. The LDA values for the E_{FB} are also included for some configurations.

Position of H_2O molecule		E_{CB}	E_{vdW}	E_{FB}	Carbon nanotube diameter	O–C separation	Buckling (%)
			(A) Inside				
1 H_2O on 1 unit cell							
(i) O at axis and $-H_2O$ plane parallel to tube axis							
Between *C* planes	GGA	0.076	0.177	0.228	8.16	4.10	0.5
	LDA	0.188	0.177	0.340			
Within a *C* plane		0.076	0.176	0.227	8.18	4.06	0.3
(ii) O at axis and $-H_2O$ plane normal to tube axis							
Between *C* planes		0.051	0.160	0.186	8.36	4.22	1.5
Within a *C* plane		0.055	0.137	0.167	8.61	4.28	1.3
(iii) 1D chain of water dimers	GGA	0.047	0.137	0.159	8.54	4.07	0.6
	LDA	0.155	0.137	0.267			
			(B) Surface				
1 H_2O on 1 unit cell							
(i) Top site							
H_2O plane normal to axis							
O toward tube	GGA	−0.046	0.138	0.067	8.36	2.82	3.2
	LDA	0.097	0.138	0.210			
(ii) Midhexagon							
H_2O plane parallel to axis							
2*H* toward tube	GGA	−0.011	0.110	0.074	8.36	3.27	1.7
	LDA	0.139	0.110	0.224			

and the O atom toward the tube surface and the corresponding LDA value is 0.287 eV.

As the lattice constant for the (5,0) tube (=4.23 Å) is greater than the above calculated equilibrium separation of 2.89 Å between the two H_2O molecules in a chain kept in vacuum, there is no significant contribution of the H_2O-H_2O interactions to the energy of the doped tube. One H_2O molecule per unit cell corresponds to an adsorbate concentration of 5%.

H_2O-doped (4,2) nanotube. We do not calculate the enhaned ΔE_{zp} for the (4,2) tube but choose a value equal to 13 meV obtained earlier for the (5,0) tube. The E_{FB} for a H_2O molecule residing on the midbond site is negative indicating no adsorption. The corresponding LDA value for E_{FB} is 0.204 eV which favors adsorption. The unit cell contains 56 C atoms, and one H_2O molecule in the unit cell corresponds to a maximum dopant concentration of about 2%.

To sum up for the small-diameter nanotubes, one observes significant E_{FB} values in GGA for the achiral armchair (3,3) and zigzag (5,0) nanotubes but negligible E_{FB} for the small-diameter chiral (4,2) nanotube. Thus, there will occur appreciable adsorption of H_2O molecules on the small-diameter achiral nanotubes in contrast to the small-diameter chiral tube.

2. Medium- and large-diameter nanotubes

H_2O-doped (6,6) nanotube. For the ZPVE contribution, we take an average of the enhanced ΔE_{zp}'s calculated for the (3,3) and (10,10) nanotubes which turns out to be 25 meV. Table I contains the various calculated parameters for the medium-diameter achiral armchair (6,6) nanotube including the E_{FB}'s obtained in GGA for one H_2O molecule lying on the various inner and surface sites, the averaged tube diameter, the averaged minimum separation between the host C atom and the O atom of the adsorbed H_2O molecule, and the tube buckling. The E_{FB}'s computed in LDA for some cases are also included in the table.

Endohedral adsorption. For the (6,6) nanotube, the E_{CB}'s for the endohedral adsorption of the polar H_2O molecules are small but positive in contrast to the negative values observed for the exohedral adsorption. The E_{FB}'s are comparatively high and are quite invariant with the location of the H_2O molecule inside the host tube. The H_2O molecule will thus not experience any significant potential barrier during its mo-

tion inside the tube. The vdW energy contributions are approximately two to three times of the chemical binding energy. The E_{FB} for the H_2O molecule having its plane parallel to the nanotube axis is higher than the E_{FB} obtained for the plane normal to the tube axis.

Water dimer containing 2-H_2O molecules. It may be recalled that an infinitely long 1D (6,6) carbon nanotube is generated by repeating its unit cell containing 24 atoms a large number of times along the tube axis depending on the computer memory. In such a case, this host tube unit cell also encapsulates the six atoms of the water dimer; there are now a total of 30 atoms in the unit cell and the repetition of this 30 atom unit cell along the tube axis will produce an infinitely long (6,6) carbon nanotube encapsulating an infinitely long 1D chain of water dimers. This chain contains the familiar O-H binding of the water but two out of the four O-H bonds seen in the bulk ice are broken here. The E_{FB} per H_2O molecule is seen to be 0.159 eV in GGA and 0.267 eV in LDA (Table I). The average of the two values is 0.213 eV.

The present result obtained for the infinite waterlike chain encapsulated inside the nanotube is expected to be applicable to a finite water chain inside a finite nanotube except for the end effects. We will see later that these end effects do not change the present results significantly. The present study shows that in vacuum, the 1D water chain is coupled to the carbon nanotube and there will be no transmission of water through the comparatively small-diameter (6,6) nanotube.

Exohedral adsorption. For the surface adsorption of the H_2O molecules, we find that the E_{CB}'s are negative and the E_{FB}'s are again quite small. The E_{FB}'s are smaller than those observed for the small-diameter achiral nanotubes discussed above. The binding is quite similar both for the top and midhexagonal sites. For the top site, the E_{FB} is 0.067 eV in GGA but 0.210 eV in LDA whereas for the midhexagonal site, the E_{FB}'s in GGA and LDA are 0.074 and 0.224 eV, respectively.

Motion of single H_2O molecule or water dimer in finite-sized (6,6) nanotube. The study of the movement of the water is of great interest. We have made an *ab initio* investigation of the motion of a single H_2O molecule and also a water dimer through a finite-length (6,6) carbon nanotube both placed in vacuum. The two open ends of the finite carbon nanotube have free electrons, which may affect the motion of the H_2O molecule or dimer.

In order to simulate the motion of the H_2O molecule or dimer, one of them was placed at the different locations with respect to the carbon nanotube on its axis starting with a location far away from one open end of the nanotube, approaching toward it, entering inside the nanotube, and finally coming out the second open end of the nanotube. At first, we start with the unpassivated carbon nanotube and later on consider the nanotube with its open ends passivated by the H atoms.

A supercell having sizes of 21–26 Å in three dimensions containing the system comprising of the H_2O molecule or dimer and the carbon nanotube was repeated periodically in the space. This dimension of the supercell was found to be adequate to avoid the interference effects between its images.

An optimization similar to the other studied systems was made for each varying position of the moving object and the energy of the system containing the (6,6) tube plus the H_2O molecule (water dimer) was obtained for the different locations of the molecule or dimer. We do not consider here the ZPVE's and take the system energy as the sum of the CBE and the vdW energies.The variation of the system energy per H_2O molecule with the location of the H_2O molecule (or dimer) for the (6,6) tube of length 6.2 Å has been depicted in Fig. 2.

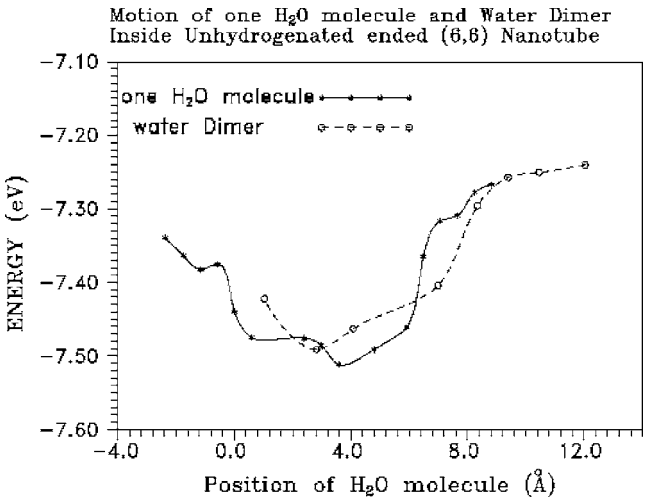

FIG. 2. Variation of the total system energy with the location of the H_2O molecule and the 2-H_2O water dimer lying on the axis of the (6,6) carbon nanotube of length of 6.2 Å either outside or inside the tube.

One observes that the system energy decreases as the H_2O molecule or the dimer approaches the nanotube and becomes minimum approximately near the open end of the tube and practically remains constant inside the nanotube. This behavior is repeated when the H_2O molecule or the dimer comes out the other open end of the tube. The H_2O molecule or the dimer is thus trapped inside the tube. We name the maximum system energy difference between the two locations of the molecule or dimer during its total journey as ΔE. This ΔE will be the potential barrier faced by the H_2O molecule or the dimer encapsulated within the nanotube placed in the vacuum to become free. For both the H_2O molecule and dimer, ΔE turns out to be about 0.25 eV.

It is well known that the open ends of a carbon nanotube possess free electron charges and they might influence the polar H_2O molecules and change the energy of the system comprising the carbon nanotube and the H_2O molecules. In our next step, we pacify the carbon atoms of both the open ends of the (6,6) carbon nanotube by the required 24 H atoms. We determine the minimum energies of the above system in the *ab initio* calculation for the two locations of the water dimer: when the dimer is encapsulated completely inside the nanotube and when the dimer lies fully outside the nanotube quite away from its open end. The difference in the energies of the system for the two locations of the dimer, ΔE for the H-passivated carbon nanotube, is seen to be 0.170 eV.

In order to see the interference effects between the images of the system comprising the nanotube and the H_2O molecules, we tested the convergence of the above calculated

TABLE II. Binding energy per H_2O molecule in eV for the adsorption of H_2O molecule in or on (10, 0) nanotube in GGA. The final binding energy, $E_{FB}=E_{CB}+E_{vdW}-\Delta E_{zp}$ ($\Delta E_{ZP}=0.028$ eV). The averaged diameter of the carbon nanotube and the separation between O and the nearest C of SWCNT in Å, and the bucklings are also included. The LDA values for the E_{FB} are also included for some configurations.

Position of H_2O molecule		E_{CB}	E_{vdW}	E_{FB}	Carbon tube diameter	O–C separation	Buckling (%)
		(A) 1 H_2O on 1 unit cell Inside					
(i)O at axis and –H_2O plane parallel to tube axis							
Between C planes	GGA	0.046	0.208	0.226	7.85	3.97	0.01
	LDA	0.207	0.208	0.387			
Within a C plane		0.044	0.208	0.224	7.86	3.91	0.01
(ii) O at axis and –H_2O plane normal to tube axis							
Between C planes		0.052	0.209	0.233	7.85	3.96	0.03
Within a C plane		0.055	0.209	0.236	7.85	3.90	0.03
		(B) 1 H_2O on 1 unit cell					
Surface top							
(i) H_2O plane normal to axis							
O toward tube							
	GGA	–0.030	0.114	0.056	7.85	2.92	0.1
	LDA	0.076	0.114	0.162	7.85	2.92	0.1
(ii) H_2O plane parallel to axis							
O toward tube		–0.073	0.114	0.013	7.85	2.92	0.1
Surface midhexagon							
(i) H_2O plane normal to axis							
O toward tube		–0.114	0.198	0.046	7.85	2.89	0.1
(ii) H_2O plane parallel to axis							
O toward tube		–0.294	0.276	–0.046	7.85	2.71	0.1

$\Delta E=0.170$ eV by increasing the size of the supercell containing the carbon nanotube plus the dimer in all the three dimension up to 26 Å. We also checked the convergence of the above value against the size of the carbon nanotube by performing a separate calculation for a larger (6,6) carbon nanotube having a length of 8.52 Å.

In vacuum, a water dimer (1-H_2O molecule) is trapped inside a finite-sized (6,6) carbon nanotube with length of 8.52 Å, and requires an energy of 0.170 eV to leave the tube at 0 K. The present finding is supported by our earlier calculation of a similar binding energy equal to 0.159 eV obtained for the infinitely long 1D chain of similar dimers encapsulated inside the infinitely long carbon nanotube in vacuum (see Table I).

The above value of $\Delta E=0.170$ eV has been obtained in GGA. The corresponding ΔE in LDA is seen to be 0.275 eV. It has been seen in some other cases such as for the adsorption of Xe atoms and CH_4 molecules on the carbon nanotube[28,29] that the available experimental values for E_{FB}'s lie in between the GGA and LDA values, and an average of LDA and GGA is seen to be quite near the experimental values. We, therefore, take an average value of ΔE which is 0.223 eV. This will be the real value which will be seen in the experiments.

H_2O-doped (10,0) nanotube. The enhanced ΔE_{zp} for the medium diameter achiral zigzag (10,0) nanotube turns out to be 28.3 meV, as shown in Table IV.

Endohedral adsorption. The various computed structural parameters are presented in Table II. The E_{FB}'s for the endohederal adsorption (Table II) for the different orientations of the polar H_2O molecule are again positive and are comparatively high ($\approx$0.23 eV) because of the occurrence of the large vdW energy arising from a large number of carbon atoms in the unit cell. Further, the E_{FB} is quite independent of the orientation of the H_2O molecule plane and its location inside the host tube. Thus, the H_2O molecule will easily move inside the carbon nanotube. The H_2O molecule incurs negligible buckling.

Exohedral adsorption. For the adsorption of the H_2O on the (10,0) tube surface, we find again, the negative values for E_{CB} but positive E_{FB}'s which are smaller than those obtained for the corresponding small-diameter zigzag (5,0) tube. The binding at the top site is somewhat stronger than on the midhexagonal site. Further, the H_2O molecule is strongly

TABLE III. Binding energy per H_2O molecule in eV for the adsorbed H_2O molecules in or on (10,10) nanotube in GGA. The final binding energy, $E_{FB}=E_{CB}+E_{vdW}-\Delta E_{zp}$ ($\Delta E_{ZP}=0.030$ eV). The averaged diameter of the carbon nanotube and the separation between O and the nearest C of SWCNT in Å, and the bucklings are also included. The LDA values for the E_{FB} are also included for some configurations.

Position of H_2O molecule		E_{CB}	E_{vdW}	E_{FB}	Carbon tube diameter	O-C separation	Buckling (%)
			(A) Inside				
(i) 1 H_2O in 1 unit cell							
H_2O plane normal to axis							
O off tube axis	GGA	0.022	0.051	0.043	13.52	4.41	0.09
	LDA	0.034	0.051	0.055			
O at tube axis		0.006	0.024	0.000	13.52	6.75	0.09
(ii) 4 H_2O in 1 unit cell		0.005	0.051	0.026	13.52	4.41	0.08
(ii) 12 H_2O in 1 unit cell		−0.456	0.350	−0.136	13.58	2.32	1.27
			(B) 1 H_2O on 1 unit cell				
Surface midhexagon							
(i) H_2O plane normal to axis							
O toward tube		−0.218	0.264	0.016	13.50	2.89	1.0
(ii) H_2O plane parallel to axis							
2*H* toward tube	GGA	−0.008	0.120	0.082	13.52	3.33	3.2
	LDA	0.150	0.120	0.240			
O toward tube		−0.250	0.266	−0.014	13.50	2.82	1.3
Surface top							
(i) H_2O plane normal to axis							
O toward tube	GGA	−0.059	0.158	0.069	13.49	2.76	0.1
	LDA	0.065	0.158	0.193			
(ii) H_2O plane parallel to axis							
O toward tube		−0.327	0.302	−0.055	13.49	2.75	0.7

bound when the H_2O plane is normal to the tube axis and the O atom lies toward the tube surface. For the top site, the E_{FB}'s in GGA and LDA are 0.056 and 0.162 eV, respectively. The exohedral adsorption will be much smaller than the endohedral adsorption.

The present prediction of the top site as the minimum-energy adsorption site has also been reported by Zhao *et al.*[26] The earlier authors have employed the localized basis (DMOL) for obtaining the equilibrium geometry and adsorption energy whereas we have used the plane-wave basis (ABINIT) for the determination of all the quantities. However, the present E_{CB} obtained in LDA (0.076) eV is smaller than a value of 0.143 eV reported by Zhao *et al.* The discrepancy in the CBE may arise because our molecule-tube separation, 2.92 Å is larger than 2.69 Å reported by Zhao *et al.*[26] It may be noted that the present vdW energy turns out to be 0.114 eV which has been ignored by earlier authors.

H_2O-*doped (10,10) nanotube*. For the large-diameter achiral armchair (10,10) carbon nanotube, the calculated enhanced ZPVE, ΔE_{zp} is obtained as 30 meV (see Table IV of the Appendix). Table III contains all the details of the various calculated parameters.

Endohedral adsorption. We have investigated the effects of the different concentrations of the H_2O molecules adsorbed inside the wide (10,10) nanotube on the E_{FB}. We observe that the binding of the H_2O molecule is large when its plane is normal to the nanotube axis. We started with the adsorption of one H_2O molecule lying on the tube axis or at off-axis positions in the single unit cell containing 40 atoms. The H_2O molecule at the off-axis site lies 2.37 Å away from the tube axis. The E_{FB}'s are seen to be quite small for each type of the endohederal adsorption (Table III). It is 0.043 eV for the off-axis position and zero for the on-axis location of the H_2O molecule. Also, the large separations of the H_2O molecule from the majority of the host C atoms give rise to quite small contribution of the vdW energy in contrast to that of the exohedral adsorption of the H_2O molecules discussed later. Surprisingly, the E_{FB} in LDA for the off-axis position of the H_2O molecule is small and equal to 0.055 eV, which is quite near to the corresponding value of 0.043 obtained in GGA.

Next, we increased the number of the H_2O molecules lying at the off-axis positions in a unit cell to four, and observe that the strength of the chemical binding of the H_2O molecule to the carbon nanotube drops drastically, i.e., $E_{CB}=0.005$ eV and $E_{FB}=0.026$ eV. Here, again each H_2O molecule is 2.37 Å away from the tube axis. One observes an attractive H_2O-H_2O interaction between the polar H_2O mol-

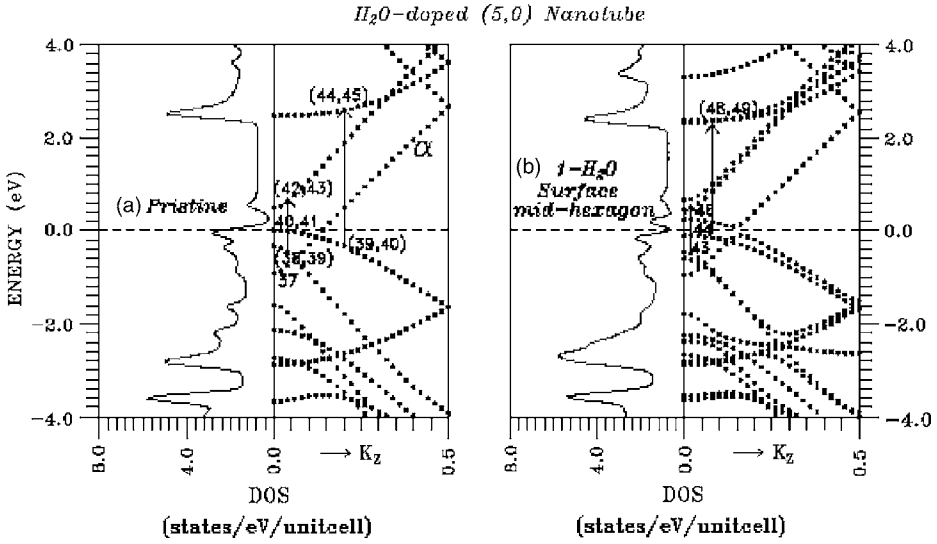

FIG. 3. Electronic structure and the density of electron states (DOS) in the vicinity of the Fermi level for the (5,0) nanotube. (a) Pristine and (b) Doped with 1-H_2O molecule on surface mid-hexagonal site. For the pristine tube, the top most filled and the lowest unfilled states have been marked as (38 to 40) and (41 to 45) near the center of the BZ. The numbering is different at various values of k_z. Some typical optical transitions have also been demonstrated.

ecules inside the unit cell and a reduced coupling to the host carbon nanotube resulting into a quite small value of E_{FB}. The size of the H_2O molecule is quite small and one may expect an accommodation of several more H_2O molecules inside the large-diameter (10,10) nanotube that will result in a smaller host C-H_2O separation and an enhancement in the resulting vdW energy. In order to check this situation, we consider 12 H_2O molecules per unit cell inside the tube and find that the E_{FB} becomes negative which rules out the endohedral adsorption of the 12 H_2O molecules per unit cell of the (10,10) carbon nanotube. One may thus infer that there will be appreciable adsorption of the H_2O molecules inside the (10,10) carbon nanotube as has been reported by Maniwa *et al.*[35]

The E_{FB}'s are again quite similar for all the locations of the H_2O molecules inside the (10,10) tube and thus there exists no potential barrier for the motion of the H_2O molecule inside the tube. This observed smoothness of the (10,10) tube for the motion of a cluster of the H_2O molecules (or water) will lead to rapid transport of H_2O gas (or water) along the tube as has been observed in recent experiments.[15,16]

Exohedral adsorption. The binding is again appreciable for the exohedral adsorption. The E_{FB} in GGA is maximum ($\approx$0.082 eV) for the midhexagonal surface site with the LDA value as 0.240 eV. The averaged E_{FB} is thus 0.161 eV.

We decreased the adsorbant concentration by placing 1-H_2O molecule on the surface-top site of the two unit cells (80 atoms) and found that the E_{FB} increases only by a few percent. This doubling of the unit cell will correspond to a maximum adsorption concentration of 1.25% on the surface. At any finite temperature, the available thermal energy may lead to quite small adsorption. Zahab *et al.*[36] have reported the surface adsorption whereas Maniwa *et al.*[35] did not find any evidence of water adsorption at the intertube channels of the bundles of the (10,10) nanotubes. Their result will also be valid for the surface adsorption.

To sum up, one finds that for the surface adsorption, the E_{FB}'s, in general, increase with the curvature of the tube. The adsorption of the H_2O molecules prefers the midhexagonal sites of all the armchair tubes and the small-diameter zigzag (5,0) tube but instead prefers the surface-top sites of the zigzag (10,0) nanotube.

B. Electronic structure

We have computed the electronic structure and the electron density of states (DOS) for the equally spaced 51, 26, 16, 11, 11, and 11 $\vec{k}$ points in the linear BZ for the (3,3), (5,0), (4,2), (6,6), (10,0), and (10,10) nanotubes, respectively. A broadening of 0.11 eV has been chosen for the DOS to avoid the spiky structure. The origin of the energy has been set either at the Fermi level (E_F) or the highest occupied state.

The point-group symmetry of a host tube is changed by the H_2O molecule lying on the off-axis position inside the nanotube or on the surface of the nanotube. This induces splitting in the electron energy states.

1. H_2O*-doped small-diameter nanotubes*

For the details of the electronic structure and the DOS for the pristine small-diameter nanotubes, we refer the reader to our earlier article.[37]

For one H_2O molecule adsorbed at the surface midhexagonal site of the (3,3) nanotube, the bonding-antibonding carbon states still cross at E_F. The states split because of the lowering of the symmetry by doping and one low-lying valence state gets mixed with the states of the H_2O molecule. The numbers of the van Hove singularities (vHs's) and their locations have been changed. In the vicinity of the E_F all the states are mainly the hybridized C(p)-O(p)-H(s,p) ones and the DOS increases from 0.34 units of the pristine tube to 0.38 units because of the squeezing of the parabolic bands.

The states of the pristine (5,0) tube also split in the doped tube because of the lower symmetry. The 'α' state hybridizes with the uppermost doubly degenerate valence state and splitting occurs (Fig. 3). One of the split valence states rises but remains below E_F, whereas the other one mixes with the α state and bends downward. The α state bends upward and an indirect gap of 0.196 eV appears making the doped tube semiconducting. In the vicinity of E_F the C(p)-O(p)-H(s,p) hybridized states are present.

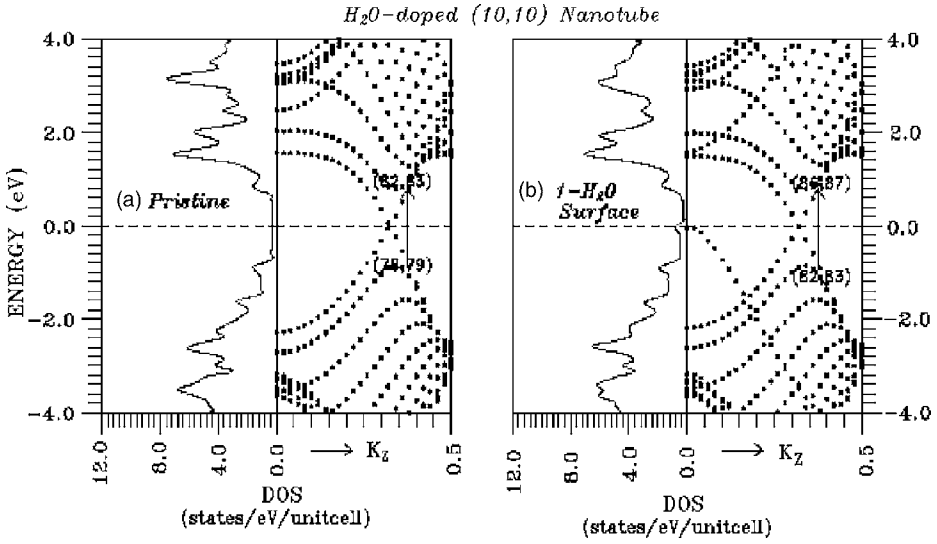

FIG. 4. Same as Fig. 3 but for the (10,10) nanotube. (a) Pristine tube. The doubly degenerate top most filled and the lowest unfilled states have been marked as (78, 79) and (82, 83) near the boundary of the BZ. Some typical optical transitions have also been drawn. (b) 1-H_2O molecule on surface midhexagonal site.

One does not observe any significant change in the electronic structure of the pristine (4,2) tube by the adsorption of the H_2O near E_F because the pristine tube already has quite a low symmetry. The valence states near the top of the valence band descend and enhance the band gap slightly from 0.14 eV seen in the pristine tube to 0.17 eV.

2. Medium- and large-diameter nanotubes

Pristine and H_2O-doped (6,6) Nanotube. For the pristine (6,6) nanotube,[38] there are larger separations between the vHs's. The separation between the two vHs's at E_F is 3.66 eV which is in agreement with that of Reich *et al.*[39] The electronic structure and DOS for the (6,6) nanotube containing a H_2O molecule inside or outside the nanotube are quite similar to that of the pristine tube except in the enhancement of the states. The locations of the states and their splitting are slightly different for the endohedral and exohedral adsorption.

(10,0) nanotube: Pristine (10,0) tube. The symmetry considerations make the pristine (10,0) tube semiconducting. No conduction state descends into the gap, a behavior different from that of the large curvature (5,0) nanotube. The gap is 0.90 eV. For details, we refer the reader to an earlier article.[28]

Doped (10,0) tube. The electronic structure and DOS for the (10,0) nanotube containing a H_2O molecule present inside or outside the nanotube are somewhat different from that of the pristine tube. Several conduction states descend and the band gap is reduced to 0.80 eV. Also, the orbital composition of the states lying in the vicinity of the E_F is seen to be quite different in the endohedral and exohedral adsorption. In the endohedral adsorption, the uppermost valence states are composed of the C(p) orbitals only, whereas in the exohedral adsorption, these valence states are the hybridized C(p)-O(s,p)-H(s,p) orbitals. On the other hand, the lowest conduction states in both the endohedral and exohedral adsorption are the hybridized C(p)-O(p-H(s,p) orbitals.

(10,10) nanotube: Pristine (10,10) nanotube. For completeness, we show the electronic structure and the DOS for the pristine achiral armchair (10,10) nanotube in Fig. 4(a). The parabolic bonding and antibonding (80,81) states cross at E_F at k_z=0.35 (Δ_F). Two saddle points appear just near Δ_F but not far away from the Δ_F, as seen in the small-diameter (3,3) nanotube. The optical transition arising from the occupied doublet (78,79) and the lowest unoccupied doublet (82,83) has been marked in Fig. 4(a). At E_F, the DOS is equal to 0.27 units.

Doped (10,10) tube: Endohedral adsorption. We show the electronic structure and the DOS for one H_2O molecule residing on the surface of the (10,10) nanotube in Fig. 4(b). The states split and some conduction states descend. The bonding-antibonding carbon states still cross at E_F. One low-lying valence state hybridizes with the H_2O states and rises upto E_F similar to the (3,3) nanotube. Both the valence and conduction states contain the hybridized C(p)-O(p)-H(p) orbitals. The DOS is enhanced to 0.78 units. We number some states which give rise to the optical absorption at the lowest energy in Fig. 4(b).

In order to see the charge transfer from the H_2O molecules to the host carbon nanotube, we depict the excess electronic charge density of the nanotube doped with 4-H_2O molecules inside the tube over that of the pristine tube in one C plane in Fig. 5. Here, the charge contours are shown in the range of 0.0–0.75 $e/(\text{a.u.})^3$ with an interval of 0.05 $e/(\text{a.u.})^3$. One observes that there exists extra electronic charge on the carbon nanotube donated by the H_2O molecules. A similar conclusion has been reported by Zhao *et al.*[26]

As there is transfer of electronic charge from the H_2O molecule to the carbon nanotube, the H_2O molecule behaves as a donor. A high concentration of the adsorbed H_2O molecules will donate more electronic charges to the tube resulting into high electric conduction, and one expects enhanced conductivity with the concentration of the H_2O molecules. The present result is in perfect concurrence with the electrical conductivity measured by Zahab *et al.*[36] performed on the SWCNT mat containing water vapor for a variable concentration of the H_2O molecules. The pristine carbon nanotube behaves as a p-type semiconductor and therefore initially for a low concentration of the H_2O molecules, the electronic charge donated by the H_2O molecules compensates the posi-

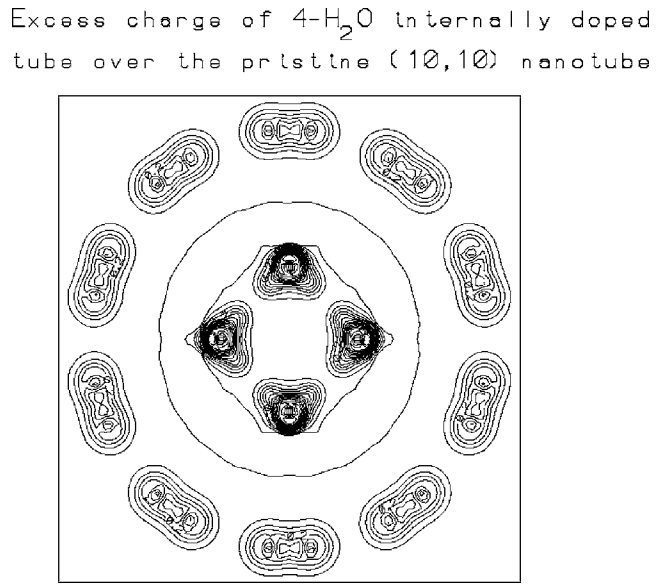

FIG. 5. The excess electronic charge density of the 4-H_2O endohedrally doped (10,10) nanotube over that of the pristine tube in one *C* plane. The charge contours are shown in the range of 0.0–0.75 $e/(\text{a.u.})^3$ with an interval of 0.05 $e/(\text{a.u.})^3$.

tive charge of the nanotube and the tube will show high resistance at small concentration as has been reported by Zahab *et al.*[36] For high concentration of the H_2O molecules, there will be large electronic charge on the carbon nanotube, which will result in high electric conduction.

C. Optical absorption

The zero-phonon optical-absorption spectra of the various H_2O-host tube systems have been computed similar to the ice nanotubes described in the accompanying article.

For the electromagnetic radiation polarized along the tube axis, the absorption for the various H_2O-tube configurations are depicted in Figs. 6 and 7. The absorption for the polarization normal to the tube axis is, in general, quite small.

1. (3,3) nanotube

The optical absorption for the pristine (3,3) nanotube along the tube axis is presented in Fig. 6(a). One observes a strong peak at 2.8 eV with a shoulder at 3.0 eV and a weak peak at 3.5 eV. The strong peak at 2.8 eV is very near to the peak measured at 3.1 eV by Lie *et al.*[40] and Liang *et al.*[41] for a mixture of 4 Å nanotubes. A peak at 2.83 eV in LDA appears in the other calculations.[42–44] Spataru *et al.*[44] considered the many-body effects and the excitonic contributions and obtained this peak at 3.17 eV that approaches the experimental value of 3.1 eV. For more details, we refer the reader to an earlier article.[37]

The peak structure for the (3,3) nanotube with one H_2O on the surface [Fig. 6(a)] is quite similar to that of the undoped tube. The edge of the strong absorption has been shifted up in the energy by 0.1 eV and this main peak at 2.9 eV originates mainly from the transitions between the filled (26–28)th and the vacant (29, 30)th states in the wave-vector range of k_z=0.4–0.48.

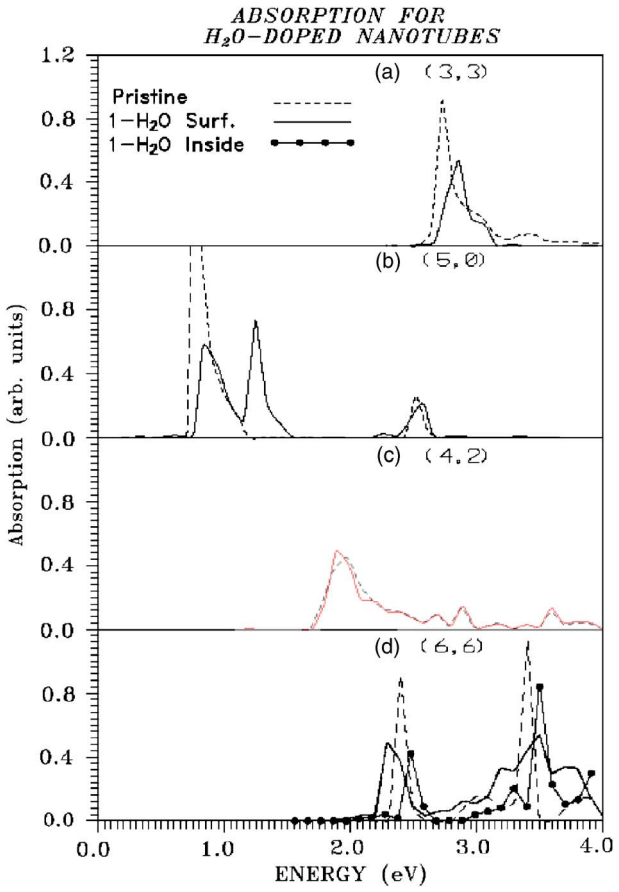

FIG. 6. (Color online) Optical-absorption spectra for the pristine and the H_2O molecule doped (a) (3,3), (b) (5,0), (c) (4,2), and (d) (6,6) carbon nanotubes in the energy range of 0–4.0 eV, respectively.

2. (5,0) nanotube

We observe that the optical absorption for the pristine (5,0) nanotube [Fig. 6(b)] contains two broad strong peaks centered at 0.8 and 2.5 eV. The absorption originates from the wave-vector range of 0.0–0.24 of k_z.

The calculated strong peaks are in reasonable agreement with the experimental peaks at 1.2, 2.1, and 3.1 eV for a mixture of 4 Å carbon tubes observed by Lie *et al.*[40] and Liang *et al.*[41] Our peaks are also near to the calculated peaks by other workers.[42,43]

We depict the absorption for 1-H_2O adsorbed (5,0) nanotube in Fig. 6(b) where one notes an extra peak at 1.25 eV along with the two strong peaks similar to the pristine tube occurring at 0.85 and 2.57 eV. The absorption at 0.85 eV originates from the transition between the occupied 43th state and the unoccupied 46th state and that at 1.25 eV from the filled 42th state and the vacant 47th state. The transitions between the occupied 44th state and the unoccupied (48, 49)th states give rise to a peak at 2.57 eV.

3. (4, 2) nanotube

The optical absorption for the pristine and the doped (4,2) nanotubes are presented in Fig. 6(c). There appear a very strong peak at 1.97 eV and several weak peaks at 2.68, 2.88,

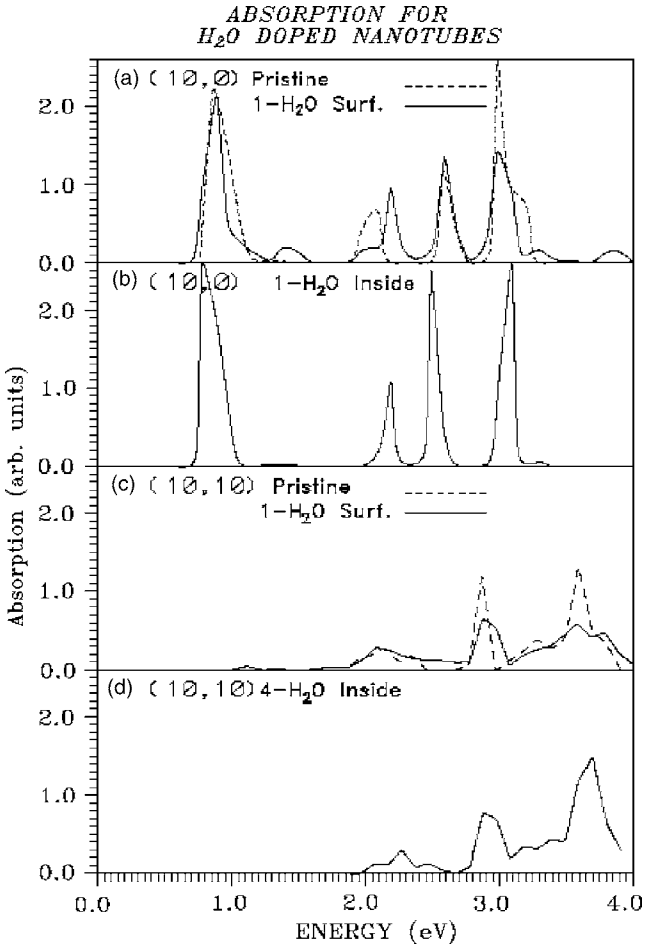

FIG. 7. Same as Fig. 6 but for the (a) pristine (10,0) nanotube and 1-H_2O molecule on surface site, (b) 1-H_2O molecule inside the (10, 0) tube, (c) pristine (10,10) nanotube and 1-H_2O molecule on surface site, and (d) 4-H_2O molecules inside the (10, 10) tube.

and 3.60 eV for the pristine tube. The present peaks are close to the measured peaks at 2.1 and 3.1 eV for a mixture of 4 Å carbon tubes obtained by Lie *et al.*[40] and Liang *et al.*[41] The other workers[42,43] have also reported the calculated peaks at 1.9, 2.9–3.0, and 3.6 eV. The case of the (4,2) tube has not been discussed by Spataru *et al.*[44] because of the big size of the unit cell.

The optical absorption for 1-H_2O on the surface of the (4,2) tube as presented in Fig. 6(c) is quite similar to that of the pristine tube. The transitions between the occupied (108–112, 115, 116)th states and the unoccupied (117, 118, 121, 122)th states mainly generate a peak at 1.89 eV.

4. (6,6) nanotube

The optical absorption for the pristine (6,6) nanotube along the tube axis as shown in Fig. 6(d) shows strong peaks at 2.4 and 3.4 eV and weak ones at 3.0 and 3.8 eV. The (6,6) nanotube has a diameter of 8.19 Å and the presently calculated peak at 2.4 eV is very close to one at 2.25 eV out of the four experimental peaks at 0.95, 1.12, 1.8, and 2.25 eV observed by O'Connell *et al.*[45] who have measured both the absorption and the emission in a mixture of SWCNTs having tube diameters lying in the range, 7–11 Å.

In Fig. 6(d), the absorption for the (6,6) nanotube having one H_2O adsorbed inside or on the surface is presented. The overall peak structure of the pristine tube is retained except for some small differences. For the endohedral adsorption, the four peaks occur at 2.5, 3.3, 3.5, and 3.9 eV, whereas for the exohedral adsorption, they appear at 2.3, 3.2, 3.5, and 3.8 eV and an extra weak peak at 2.9 eV.

The optical absorption for the 1D chain of the water dimers present inside the (6,6) nanotube is found to be quite similar to that of the pristine (6,6) nanotube except for small differences.

5. (10,0) nanotube

For the pristine (10,0) nanotube, the optical absorption in the wave-vector range, k_z=0.0–0.03 is presented in Fig. 7(a). Four strong peaks are seen at 0.87, 2.08, 2.58, and 3.00 eV. Compared to the (5,0) tube the number of peaks here has been doubled and two extra peaks appear at 2.1 and 3.0 eV.

The (10,0) nanotube has a diameter of 7.85 Å and the presently calculated two peaks at 0.87 and 2.08 eV are very close to the experimental peaks at 0.95, 1.12, 1.8, and 2.25 eV seen by O'Connell *et al.*[45] who have measured both absorption and emission in a mixture of SWCNTs having tube diameters in the range, 7–11 Å.

The calculated absorption for the H_2O lying above the top site of the (10,0) nanotube is presented in Fig. 7(a). There appear four strong peaks at 0.89, 2.19, 2.59, and 3.0 eV. Three peaks appearing at 0.89, 2.1, and 3.0 eV are similar to those seen in the host tube, whereas the peak at 2.08 eV of the pristine tube is shifted to the higher-energy side by 0.1 eV only. There also occur several extra quite weak peaks. The transitions between the (83, 84)th and the (85, 86)th states generate the peak at 0.89 eV whereas the transitions between the (81,82)th and the (92, 93)th states produce peak at 2.19 eV. The peak at 2.59 eV originates from the transitions between the (78, 79)th and the (90, 91)th states, and at 3.0 eV from the (74–78)th and the (87–89)th states.

For the endohedral adsorption, the optical absorption is presented in Fig. 7(b). The overall four strong peak structure is seen except for some changes in the locations and the relative intensities of some peaks. The peaks now appear at 0.79, 2.19, 2.49, and 3.09 eV.

6. (10,10) nanotube

We present the optical absorption for the pristine (10,10) nanotube along the tube axis in Fig. 7(c). The weak broad absorption is seen around 2.15 and 3.28 eV and the strong one in the energy range, 2.8–4.0 eV. Two strong peaks appear at 2.87 and 3.59 eV. The presently predicted two peaks at 2.15 and 2.87 eV are among the four experimental peaks observed at 0.7, 1.3, 1.9, and 2.6 eV in the mixture of the SWCNT's of 14 Å diameter by Hwang *et al.*[46] The experimental peaks at 1.2, 1.8, and 2.4 eV in a mixture of the isolated and the bundles of tubes having diameters in the range of 12–16 Å have also been reported by Kazaoui *et al.*[47] Liu *et al.*[48] have observed variation in the locations of the peaks with the tube diameter in the range, 9–14 Å in the bundles of the tubes. In all the above experiments, a peak at

0.7 eV has been reported which is not predicted by our calculation for the pristine (10,10) nanotube. The tubes of other chiralities possessing similar diameter may be responsible for this peak. We have predicted a peak structure near 3.59 eV not yet reported in the literature.

In Fig. 7(c), we depict the absorption for the (10,10) nanotube having one H_2O adsorbed at any surface site. The weak multiple peak structure at 2.15 eV of the pristine tube merges into a broader peak which extends up to the next broad peak at 2.88 eV. One peak of the pristine tube appearing at 3.59 eV is retained but with reduced intensity. A new peak appears at 3.79 eV. The occupied (75–78)th and the unoccupied (85–91)th states produce strong absorption in the energy region, 2.7–4.0 eV.

The peak structure for the endohedral adsorption of 4 H_2O molecules is shown in Fig. 7(d) which is more near to that of the pristine tube except for the broadening of all the peaks and some extra structure with some changes in the locations and the relative intensities of the high-energy peaks.

IV. DISCUSSION

In the present investigations, two different types of the *ab initio* calculations have been performed for a system containing a (6,6) carbon nanotube and a water dimer made up of two H_2O molecules arranged in a water chainlike structure placed in vacuum. In one case, a single water dimer is placed at various locations at the axis of a finite carbon nanotube of length, 8.52 Å whereas in the other case, an infinite 1D chain of similar dimers is encapsulated inside an infinite carbon nanotube.

For the first case, one obtains a value of ΔE equal to 0.223 eV which is the average of its GGA and LDA values and is expected to be near to the experimental value, as discussed above in the text. The energy of the dimer is lower by an amount of ΔE when it lies inside the (6,6) carbon nanotube than its energy when it is far away from the carbon nanotube and is independent of the tube. ΔE is the energy which will be released by the dimer when entering the carbon nanotube and also the energy needed by the dimer to come out of the carbon nanotube.

In the other case studied, an infinitely long waterlike 1D chain of water dimers is encapsulated inside an infinitely long (6,6) carbon nanotube in vacuum. The E_{FB} per H_2O molecule is seen to be 0.159 eV in GGA and 0.267 eV in LDA (Table I). The average of the two values is 0.213 eV. This is the binding energy of the H_2O molecule when present inside the carbon nanotube and is the energy needed by the H_2O molecule to be free of the carbon nanotube. This energy is quite similar to the energy, ΔE equal to 0.223 eV required by the molecule to get itself free in the first case.

It is remarkable that quite similar values for the binding energy for the H_2O molecule are obtained for the two quite different systems where in one case, there is a finite carbon nanotube of length of 8.52 Å and in the other case, an infinitely long (6,6) carbon nanotube has been employed. It points toward the fact that the end effects are not very significant and the choice of a carbon nanotube of finite length does not influence our conclusions.

As discussed earlier, the water dimer will need an averaged value of ΔE=0.223 eV to free itself from the medium-sized (6,6) carbon nanotube placed in the vacuum. This energy will not be available as thermal energy at any temperature. One may thus infer that when the nanotube and the H_2O molecule or the dimer are placed in the vacuum one may not see any transmission of the H_2O molecules or water dimer through the (6,6) carbon nanotube.

The situation may be different in case the two open ends of the (6,6) carbon nanotube is immersed either in the liquid water or the water vapor at high vapor pressure. The energy of the liquid water is lower as compared to a free H_2O molecule by about 0.25 eV, which is quite near to ΔE =0.22 eV, the binding energy of the dimer in the carbon nanotube. Thus, at high temperatures when the sufficient thermal energy is available to the H_2O molecules or dimer, the water transport may occur through the carbon nanotube via the random water dissociation at one end and random association at the other end of the nanotube.

A similar 1D water chain inside a finite carbon (6,6) tube has been discussed by Hummer *et al.*[3] using computer simulation with similar conclusions for the carbon tube immersed in the water.

In the literature, there are different reports about the relative magnitudes of the binding energies of the adsorbates on the carbon nanotubes calculated in the LDA and GGA.

We compare here the binding energies calculated in the LDA and GGA for the various H_2O-carbon nanotube configurations. In the majority of the H_2O-doped cases, we observe that for any system, the calculated E_{CB} in LDA is seen to be near to E_{FB} obtained in GGA. For the endohedral adsorption, the LDA E_{CB}'s are always smaller than the GGA E_{FB}'s, whereas for the exohedral adsorption, the reverse is true except for the surface-top adsorption of the H_2O molecule on the (10,10) nanotube. It may be reminded that in the calculation of E_{FB} obtained in GGA, the vdW energy has been included. It is unfortunate that no experimental data for the binding energies are available for the H_2O-doped carbon nanotubes except a finding by Maniwa *et al.*[35] who have reported no adsorption of the H_2O molecules on the surface of the (10,10) carbon nanotubes. The presently calculated maximum E_{FB} for the surface adsorption on the (10,10) carbon nanotube in GGA is 0.082 eV, which is quite small to give rise to any appreciable adsorption in concurrence with the experimental observation of no surface adsorption. The corresponding calculated LDA value, E_{CB} after ignoring the vdW energy is 0.147 eV, which is double of the E_{FB} obtained in GGA and, therefore, in a LDA calculation one will expect appreciable H_2O adsorption on the surface of the (10,10) carbon tube in disagreement with the experimental observation. Thus, the LDA binding energies for the H_2O molecules on the surface of the (10,10) carbon nanotubes seem to be large and it seems to be the case of overbinding of the adsorbates to the carbon nanotubes.

We now look for other adsorption cases available for the carbon nanotubes where some measured data for the binding energies are available. Earlier, we have investigated two such cases: the carbon nanotube doped with the inert Xe atoms[28] or with the inert CH_4 molecules.[29] Similar to the H_2O-doped carbon nanotubes, it has been observed that in a majority of

the studied Xe and CH_4-doped carbon nanotubes, the LDA E_{CB} values without including the vdW energies are close to the GGA E_{FB} values which include the vdW energies. However, there are several exceptions to this observation in the Xe-doped carbon nanotubes where the E_{CB} values in LDA are much smaller than the E_{FB} values in GGA.

We now focus on the binding of the different types of the adsorption on the experimentally studied (10,10) carbon nanotubes. In the case of the (10,10) carbon nanotube doped with the Xe atoms, it has been observed[28] that the E_{FB} in GGA is 0.315 eV and E_{CB} in LDA is 0.207 eV as compared to the measured values of 0.26–0.28 eV. The experimental value thus lies in between the two values, and therefore the estimation of the binding energies both in LDA and GGA with vdW energy is essential to reach the experimental observation.

For the CH_4-doped (10,10) carbon nanotube,[29] the computed E_{FB} in GGA is-0.003 eV, whereas E_{CB} in LDA is 0.24 eV against the experimental value of 0.133 eV. It is thus evident that E_{CB} in LDA cannot account for the measured value of 0.133 eV. The corresponding vdW energy is seen to be 0.232 eV. An average of the E_{FB}'s calculated in GGA and LDA turns out to be 0.110 eV, which is near the experimental value. One may thus conclude that in this system, the experimental value cannot be understood theoretically without the inclusion of the vdW energy.

We now compare the E_{FB}'s, obtained for the H_2O and CH_4 molecules adsorbed inside the (10,10) carbon nanotube. In GGA, the calculated E_{FB}'s for the H_2O and CH_4 molecules are 0.043 and 0.080 eV, respectively, which predict a stronger coupling of the CH_4 molecules to the (10,10) carbon nanotube than that of the H_2O molecules. Also, we have seen above that the average of the LDA and GGA values of E_{FB} is seen to be nearer to the experimental value wherever available. These averaged E_{FB}'s for the CH_4 and H_2O-doped nanotubes are 0.110 and 0.049 eV, respectively, which again reveal two times stronger binding of the CH_4 molecules than the H_2O molecules.

Quite recently, Maniwa *et al.*[49] have studied the electrical resistivities of the gases absorbed inside the carbon SWCNTs containing ice and water. They have assigned an increase in resistivity to the occupation of the CH_4 gas in place of the water inside the carbon nanotube. As discussed above, the binding energy of the CH_4 molecule to the carbon nanotube is higher as compared to that of the H_2O molecule, the occupation of the carbon nanotube by the CH_4 molecules after ejecting out the H_2O molecules will be observed in the experiments as has been reported by Maniwa *et al.*[49]

The above discussion shows the importance of the calculations both in LDA and GGA along with the vdW energies and the zero-point energies to find any realistic estimation of the binding energies to be observed in the experiments.

V. CONCLUSIONS

Our *ab initio* study shows that in vacuum, a water dimer or 1-H_2O molecule is trapped inside the finite-sized medium diameter (6,6) carbon nanotube and needs an energy of about 0.223 eV to come out of the open end of the carbon nanotube. We also observe that an infinitely long 1D chain of H_2O molecules or dimers is also strongly bound inside an infinitely long carbon nanotube with a binding energy of 0.213 eV. The real system in practice will lie somewhere between the above discussed two extreme systems; one of them is a small-sized system containing both small-sized water chain and the carbon nanotube, and the other one has infinitely long 1D chain of dimers encapsulated inside the infinitely long carbon nanotube. The energy of the dimer inside the carbon nanotube will be lower than its energy outside the nanotube by about 0.223 eV and no transmission of the dimers is expected in vacuum.

The situation will be different in case the two open ends of the carbon nanotube is immersed either in the liquid water or the water vapor at high vapor pressure at high temperatures where one may observe the transmission of the water dimers through the carbon nanotube via the random water dissociation at one end and random association at the other end of the nanotube.

In vacuum, quite strong binding is seen for the H_2O molecules encapsulated inside the medium diameter (6,6) and (10,0) carbon tubes resulting into no transmission of the H_2O molecules or the water through them. On the other hand, there is weak coupling of the H_2O molecules with the (10,10) carbon tube. The H_2O molecules or the water will easily flow through the large-diameter nanotubes even in vacuum in concurrence with the recent experiments. Appreciable endohedral and exohedral adsorption will be observed in/on the (10,10) carbon tube in agreement with the experiments.

The adsorption of the water molecules is caused by the dispersion forces, i.e., the vdW interactions. The role of the vdW interactions in the estimation of the BE for the weakly bound adsorbates cannot be ignored as has been done in several earlier publications. In our earlier studies of the adsorption of the inert Xe atom[28] and the inert molecule CH_4 (Ref. 29) where the experimental data were available, we observed that the LDA overbinds the H_2O molecule and the GGA underbinds it, and for a reliable theoretical estimate, one might take an average of the E_{FB}'s determined in LDA and GGA.

One observes chirality-dependent binding of the H_2O molecules on the carbon nanotubes and finds comparatively strong adsorption on the small-diameter achiral carbon nanotubes in contrast to very weak adsorption on the chiral (4,2) nanotube. The adsorption is preferred on the midhexagonal sites of all the achiral nanotubes except for the achiral (10,0) nanotube where the surface-top site is preferred. The small (medium-sized) diameter tubes will strongly adsorb (accommodate) the water molecules outside (inside) the nanotubes.

The adsorption of the H_2O molecules incurs small changes in the diameters of the nanotubes. However, large buckling is seen in the small-diameter tubes in contrast to negligible buckling in the large-diameter tubes.

The present article shows the importance of the calculations both in LDA and GGA along with the vdW energies and the zero-point energies to find any realistic estimation of the binding energies to be observed in the experiments.

In the electronic structure of the doped tube, splitting in the states occurs in the whole energy range. The effects are

TABLE IV. Zero-point vibrational energies (ZPVEs) and the enhanced ΔE_{zp} in meV for the different H_2O-nanotube configurations.

	ZPVE								
	$(\vec{q}=0,0,0)$				$(\vec{q}=0,0,0.5)$				
Nanotube	Undoped nanotube	Isolated H_2O	Doped nanotube	ΔE_{zp}	Undoped nanotube	Isolated H_2O	Doped nanotube	ΔE_{zp}	Average ΔE_{zp}
(3,3)	974.7	658.0	1668.2	35.5	928.4	747.8	1682.4	6.2	20.9
(5,0)	1160.5	601.7	1800.0	37.8	1223.4	625.5	1836.0	−12.9	12.5
(10,0)	1653.0	658.1	2372.0	60.9	1717.0	751.3	2464.0	−4.3	28.3
(10,10)	1724.0	659.8	2417.5	33.7	1851.8	749.1	2627.1	26.2	30.0

quite significant in the large curvature tubes. The H_2O doping converts the conducting small-diameter zigzag (5,0) tube into a semiconductor. The adsorption of the H_2O molecule reduces the band gap of a semiconducting achiral zigzag nanotube whereas it enhances the band gap of a chiral semiconducting tube. The adsorbed H_2O molecules provide additional channels inside or outside the nanotube for larger electric conduction. The adsorbed H_2O molecules show a *p*-like character donating electronic charge to the nanotubes and increase the electrical conductivity with the concentration of the H_2O molecules as has been confirmed by Zahab *et al.*[36] by their measurements.

Most of the calculated peaks in the optical absorption of the large-diameter pristine (10,0) and (10,10) nanotubes have been observed in a number of experimental measurements. The adsorption of the H_2O molecules on all the tubes does not alter significantly the overall peak structures seen in the optical absorption of the pristine tubes except the (5,0) nanotube. Energy locations and the relative intensities of the peaks are altered in the achiral tubes.

ACKNOWLEDGMENTS

The authors thank the University Grants Commission, New Delhi, and the Defence Research Development Organization, New Delhi, for financial assistance and P. S. Yadav for providing the computational facilities.

APPENDIX

The atomic motions of the adsorbed H_2O molecule alongwith all the nearest-neighboring and the next-nearest-neighboring host C atoms are considered for each system within an *ab initio* pseudopotential theory. We calculate the phonon energies at the two symmetric points of the BZ ($\vec{q}=0,0,0$) lying at the center of the BZ and another at the boundary of BZ ($\vec{q}=0.0,0.0,0.5$). We perform the above computations for the doped carbon nanotube, pristine carbon nanotube, and isolated H_2O chain or chains for the various H_2O molecule-carbon nanotube configurations and obtain the enhanced zero-point energy, $\triangle E_{zp}$ after employing Eq. (5) of the text.

One H_2O molecule in the unit cell will produce nine phonon modes. The frequencies of the modes have been computed for all the atoms in the unit cell and the averaged values for them have been taken. The ZPVE's for the various H_2O-carbon nanotube configurations have been presented in Table IV.

[1] M. L. Zeidel, S. V. Ambudkar, B. L. Smith, and P. Agre, Biochemistry **31**, 7436 (1992).
[2] B. Sakmann, J. Patlak, and E. Neher, Nature (London) **286**, 71 (1980).
[3] G. Hummer, J. C. Rasalch, and J. P. Noworyta, Nature (London) **414**, 188 (2001).
[4] M. Wilkstrom, Curr. Opin. Struct. Biol. **8**, 480 (1998).
[5] M. Schlapbach and M. Zuttel, Nature (London) **414**, 353 (2001).
[6] M. Hirscher, M. Becher, M. Haluska, A. Quintel, V. Skakalova, Y. M. Choi, U. Dettlaff-Weglikowska, S. Roth, I. Stepanek, P. Bernier, A. Leonhardt, and J. Fink, J. Alloys Compd. **330**, 654 (2002).
[7] J. Kong, N. R. Franklin, C. W. Zhou, M. G. Chapline, S. Peng, K. J. Cho, and H. J. Dai, Science **287**, 622 (2000).
[8] P. G. Collins, K. Bradley, M. Ishigami, and A. Zettl, Science **287**, 1801 (2000).
[9] G. U. Sumanasekera, C. K. W. Adu, S. Fang, and P. C. Eklund, Phys. Rev. Lett. **85**, 1096 (2000).
[10] Y. Saito, T. Nishiyama, T. Kato, S. Kondo, T. Tanaka, J. Yotani, and S. Uemura, Mol. Cryst. Liq. Cryst. Sci. Technol., Sect. A **387**, 303 (2002).
[11] M. Shim, N. W. S. Kam, R. J. Chen, Y. M. Li, and H. J. Dai, Nano Lett. **2**, 285 (2002).
[12] S. C. Tsang, Y. K. Chen, P. J. F. Harris, and M. L. H. Green, Nature (London) **372**, 159 (1994).
[13] P. M. Ajayan, T. W. Ebbesen, T. Ichihashi, S. Ijima, K. Tanigaki, and H. Hiura, Nature (London) **362**, 522 (1993).
[14] D. Z. Guo, G. M. Zhang, Z. X. Zhang, Z. Q. Xue, and Z. N. Gu, J. Phys. Chem. B **110**, 1571 (2006).
[15] M. Majumdar, N. Chopra, R. Andrews, and B. J. Hinds, Nature (London) **438**, 44 (2005).
[16] J. K. Holt, H. G. Park, Y. Wang, M. Stadermann, A. B. Artyukhin, C. P. Grigoropoulous, A. Noy, and O. Bakajin, Science **312**, 1034 (2006).

[17] T. Werder, J. H. Walther, R. L. Jaffe, T. Halicioglu, and P. Koumoutsakos, J. Phys. Chem. B **107**, 1345 (2003).
[18] A. Pertsin and M. Grunze, J. Phys. Chem. B **108**, 1357 (2004).
[19] E. B. Mackie, R. A. Wolfson, L. M. Arnold, K. Lafdi, and A. D. Migone, Langmuir **13**, 7197 (1997).
[20] S. E. Weber, S. Talapatra, C. Journet, A. Zambano, and A. D. Migone, Phys. Rev. B **61**, 13150 (2000).
[21] S. Talapatra, A. Z. Zambano, S. E. Weber, and A. D. Migone, Phys. Rev. Lett. **85**, 138 (2000); S. Talapatra and A. D. Migone, Phys. Rev. B **65**, 045416 (2000).
[22] M. Muris, N. Dufau, M. Bienfait, N. Dupont-Pavlovsky, Y. Grillet, and J. P. Palmari, Langmuir **16**, 7019 (2000).
[23] M. C. Gordillo and J. Marti, Chem. Phys. Lett. **329**, 341 (2000).
[24] J. H. Walther, R. Jaffe, T. Halicioglu, and P. Koumoutsakos, J. Phys. Chem. B **105**, 9980 (2001).
[25] M. C. Gordillo and J. Marti, Phys. Rev. B **67**, 205425 (2003).
[26] J. Zhao, A. Buldum, J. Han, and J. P Lu, Nanotechnology **13**, 195 (2002).
[27] D. J. Mann and M. D. Halls, Phys. Rev. Lett. **90**, 195503 (2003).
[28] B. K. Agrawal, S. Agrawal, and S. Singh, J. Phys.: Condens. Matter **17**, 2085 (2005).
[29] B. K. Agrawal, S. Agrawal, S. Singh, and R. Srivastava, J. Phys.: Condens. Matter **18**, 4649 (2006).
[30] S. Dag, O. Gulseren, T. Yildirim, and S. Ciraci, Phys. Rev. B **67**, 165424 (2003).
[31] B. K. Agrawal, S. Agrawal, and R. Srivastava, J. Phys.: Condens. Matter **16**, 1467 (2004).
[32] T. A. Halgren, J. Am. Chem. Soc. **114**, 7827 (1992).
[33] J. P. Perdew, K. Burke, and M. Ernzerhof, Phys. Rev. Lett. **77**, 3865 (1996).
[34] A. D. Becke, Phys. Rev. A **38**, 3098 (1988); C. Lee, W. Yang, and R. G. Parr, Phys. Rev. B **37**, 785 (1988).
[35] Y. Maniwa, H. Kataura, M. Abe, S. Suzuki, Y. Achiba, H. Kira, and K. Matsuda, J. Phys. Soc. Jpn. **71**, 2863 (2002).
[36] A. Zahab, L. Spina, P. Poncharal, and C. Marliere, Phys. Rev. B **62**, 10000 (2000).
[37] B. K. Agrawal, S. Agrawal, R. Srivastava, and S. Singh, Phys. Rev. B **70**, 075403 (2004).
[38] B. K. Agrawal, S. Agrawal, and R. Srivastava, J. Phys.: Condens. Matter **15**, 6931 (2003).
[39] S. Reich, C. Thomsen, and P. Ordejon, Phys. Rev. B **65**, 155411 (2002).
[40] Z. M. Li, Z. K. Tang, H. J. Liu, N. Wang, C. T. Chan, R. Saito, S. Okada, G. D. Li, J. S. Chen, N. Nagasawa, and S. Tsuda, Phys. Rev. Lett. **87**, 127401 (2001).
[41] W. Liang, G. Chen, Z. Li, and Z. K. Tang, Appl. Phys. Lett. **80**, 3415 (2002).
[42] M. Machon, S. Reich, C. Thomsen, D. Sanchez-Portal, and P. Ordejon, Phys. Rev. B **66**, 155410 (2002).
[43] H. J. Liu and C. T. Chan, Solid State Commun. **125**, 77 (2003).
[44] C. D. Spataru, S. Ismail-Beigi, L. X. Benedict, and S. G. Louie, Phys. Rev. Lett. **92**, 077402 (2004).
[45] M. J. O'Connell, S. M. Bachilo, C. B. Huffman, V. C. Moore, M. S. Strano, E. H. Haroz, K. L. Rialon, P. J. Boul, W. H. Noon, C. Kittrell, J. Ma, R. H. Hauge, R. B. Weisman, and R. E. Smalley, Science **297**, 593 (2002).
[46] J. Hwang, H. H. Gommans, A. Ugawa, H. Tashiro, R. Haggenmueller, K. I. Winey, J. E. Fischer, D. B. Tanner, and A. G. Rinzler, Phys. Rev. B **62**, R13310 (2000).
[47] S. Kazaoui, N. Minami, H. Yamawaki, K. Aoki, H. Kataura, and Y. Achiba, Phys. Rev. B **62**, 1643 (2000).
[48] X. Liu, T. Pichler, M. Knupfer, M. S. Golden, J. Fink, H. Kataura, and Y. Achiba, Phys. Rev. B **66**, 045411 (2002).
[49] Y. Maniwa, K. Matsuda, H. Kyakuno, S. Ogasawara, T. Hibi, H. Kadowaki, S. Suzuki, Y. Achiba, and H. Kataura, Nat. Mater. **6**, 135 (2007).